Available online at www.sciencedirect.com
SCIENCE DIRECT®
Coordination Chemistry Reviews 248 (2004) 245–260
COORDINATION CHEMISTRY REVIEWS
www.elsevier.com/locate/ccr

Review

Tungsten-183 nuclear magnetic resonance spectroscopy in the study of polyoxometalates

Ya-Guang Chen*, Jian Gong, Lun-Yu Qu

Faculty of Chemistry, Northeast Normal University, Changchun 130024, PR China

Received 28 July 2003; accepted 7 November 2003

Contents

Abstract

This review focuses on the tungsten-183 NMR spectroscopy of polyoxotungstates. The ^{183}W nuclide is the only NMR-active natural tungsten isotope with a spin of 1/2 and natural abundance of 14.3%. It gives rise to very narrow resonance lines. The NMR spectral envelope depends on the structure and symmetry of the anion. The ^{183}W chemical shifts are sensitive to their surrounding environment, including central atom, electric charge and size of adjacent elements, counterions in solution and solvent. The replacement of ligand atoms in an anion by the quadrupolar vanadium nucleus or by paramagnetic ions either in a ligand site or in the central site cause the resonance signals of

* Corresponding author. Tel.: +86-431-5665252.
E-mail address: chenyg146@nenu.edu.cn (Y.-G. Chen).

0010-8545/$ – see front matter
doi:10.1016/j.cct.2003.11.003

the tungsten atoms adjacent to the substituted atoms to shift dramatically and broaden or even disappear. The spectral envelope, relative intensity of the lines and homonuclear and heteronuclear coupling constants provide the basis to identify anionic structure. Tungsten-183 NMR spectroscopy including 2-D COSY and 2-D INADEQUATE spectroscopy are used to distinguish new synthetic species, to examine product purity, to differentiate isomers and to establish new structures in solution as well as to monitor the progress of reaction. Tungsten-183 NMR spectroscopy has already become a powerful routine tool of structural characterization for polyoxotungstates in solution.

Keywords: Tungsten-183 NMR; Coupling constant; Chemical shift; Polyoxotungstates

1. Introduction

The first observation of a tungsten-183 NMR spectrum was made by Klein and Happe [1] in 1961 when the spectrum of WF_6 was indirectly recorded using a double resonance technique. In the following 20 years, ^{183}W NMR spectroscopy was used for the study of the high oxidation state compounds, WCl_6, WO_4^{2-} [2], $WF_n(OR)_{6-n}$ [3], and low oxidation state compounds, $CpW(CO)_3X$ (X = Cl, Br, I, Me) [4], $W(CO)_{6-n}[POMe]_n$ [5]. Towards the end of 1970s, Baker and co-workers [6] introduced ^{183}W NMR spectroscopy into the study of polyoxometalates (POMs). Since then a number of tungsten NMR papers have dealt with POMs involving the direct observation of W nuclide thanks to the development of commercial pulsed Fourier transform broad band spectrometers and superconducting solenoid magnets.

POMs are coordination compounds containing more than two metal atoms, which are generally formed from simple inorganic salts via condensation [7]. POMs are constructed from octahedral MO_6 and/or tetrahedral XO_4 basic structural units by sharing the edges or the vertex of the octahedron and/or the tetrahedron. An anion $PW_{12}O_{40}^{3-}$ (Fig. 1) can be obtained by acidifying the mixed solution of phosphate and tungstate with a molar ratio of 1:12. The P atom is called the central atom, while the W atoms are called the ligand atoms which are coordinated octahedrally by oxygen atoms and can be substituted by other metal atoms. Three WO_6 octahedra form a triplet W_3O_{13} by sharing octahedral edges, and four such triplets share the octahedral vertexes and arrange tetrahedrally around the central atom P, that is, the three-fold shared oxygen atoms in the triplet W_3O_{13} are coordinated to a P atom, resulting in a T_d symmetric polyoxometalate. More than 70 elements in the periodic table may act as the constituents of POMs. V, Mo and W are the principal constituents.

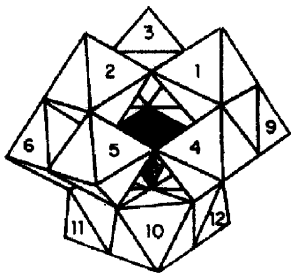

Fig. 1. Polyhedral representation of α-Keggin anion with IUPAC numbering.

The POMs have many "value-adding properties" [8], such as large size (diameter of 6–25 Å), high molecular mass (10^3–10^4 g/mol), high anionic charge (−3 to −20), discrete structure and discrete size (compared with the metallic oxides), strong electrolyte ($pK_a < 0$ in acid form), photoreducible and chemoreducible, acid forms very soluble in H_2O and other oxygen-carrying solvents (ether, alcohols, ketones), etc. It is these "value-adding properties" that make the POMs of considerable value in quite diverse disciplines of science and technology, e.g., catalysis, medicines, and materials science [8–11]. At present, the POMs continue to attract much scientific attention.

There are many nuclides detectable by NMR spectroscopy in POMs (^{11}B, ^{17}O, ^{27}Al, ^{29}Si, ^{31}P, ^{51}V, ^{71}Ga, ^{77}Se, ^{95}Mo, ^{95}Nb, ^{183}W, ^{125}Te, ^{195}Pt and so on) [7]. Some nuclides, such as B, P, Si act as the central atom; some act as ligand atoms (Mo and W), and others can act either as central atoms or as ligand atoms (V, Al, Ga, Fe, Co, etc.). However, relatively few POMs containing these elements have been studied, as yet, by NMR spectroscopy. The oxygen element is an essential constituent of POMs, but due to the low abundance (0.04%) of the nuclide ^{17}O, it is necessary to enrich the ^{17}O nuclide or carry out an ^{17}O-exchange reaction in ^{17}O-enriched water in order to obtain the ^{17}O NMR spectra of POMs. This can lead to problems in the relative quantitation of the oxygen sites [12] and restricts the application of ^{17}O NMR spectroscopy. However, the enhanced sensitivity of modern high-field NMR spectrometers provides the possibility to accumulate, quite rapidly, good signal-to-noise ^{17}O NMR spectra at the natural abundance of ^{17}O in 10–15 min after dissolution although a concentration of about 1 mol/l is required [12,13]. The ^{95}Mo nuclide with a natural abundance of 15.7% and a resonance frequency of 13.035 MHz at 4.7 T has a favorable receptivity. However, the number of reports concerning ^{95}Mo NMR study on POMs is much smaller than those concerning ^{183}W NMR because of the large electric quadrupole moment (0.12×10^{28} m^2) of the former nuclide, which results in excessively broad resonance lines in some cases. ^{183}W NMR spectroscopy is the most widely applied technique in the investigation of POMs and has become a powerful routine method for the structural characterization of POMs in solution.

2. The ^{183}W nuclide

The ^{183}W nuclide is only NMR-active isotope in natural tungsten, a transition metal element lying in the sixth period, and has a spin of 1/2, so its resonance lines are generally very narrow. But its low resonance frequency of 8.325 MHz at 4.7 T and natural abundance of 14.3% result in a low receptivity of 0.059 which makes the observation of ^{183}W signals difficult in many cases. In practice, a concentrated sample solution (~1 mol/l) and long acquisition time are necessary. A saturated solution of sodium tungstate is recommended as chemical shift reference. The ^{183}W chemical shifts span ca. 8000 ppm and a rough trend is apparent with the oxidation states. The higher oxidation state compounds are found at lower field and the lower oxidation state compounds are found at higher field [14,15].

3. ^{183}W NMR spectrum

3.1. Origin of chemical shift

The chemical shift of diamagnetic systems in solution arises from two contributions: diamagnetic (σ_d) and paramagnetic (σ_p) [15]. The diamagnetic term σ_d of the atom being considered is determined by the potential created by the inner electrons, and it is usually reasonably constant for closely related molecules. The paramagnetic term σ_p arises from the lack of spherical symmetry of the electric potential. For transition metals, the variation of the observed chemical shifts is most often dominated by the paramagnetic term σ_p, since the valence electrons of transition metal atoms occupy p, d and f orbitals with non-zero intrinsic angular moments, giving rise to a large deviation from spherical symmetry. For polyatomic ions and molecules, σ_p may be estimated from the Jameson and Gutowsky equation [16]:

$$\sigma_p = \frac{2e^2h^2}{3m^2c^2\Delta E}\left[\left\langle\frac{1}{r^3}\right\rangle_p P_u + \left\langle\frac{1}{r^3}\right\rangle_d D_u\right] \quad (1)$$

where P_u and D_u represent, respectively, the "unbalance" of valence electrons in p and d orbitals centered on the atom. ΔE is the average energy of excitation to a state of the correct symmetry to be mixed with the ground state and is often given by the lowest energy UV-Vis absorption maximum. $\langle 1/r^3\rangle_{p,d}$ represents the average value of r^{-3} over the p and d wave functions. The chemical shift δ is proportional to σ_p of the atom considered. Acerete et al. [17] examined the chemical shifts of 12-tungsto POMs and they found a straight line correlation between the ^{183}W chemical shift and the reciprocal energy, $E_{(LCT)}$, of the lowest charge transfer (LCT). A least-squares extrapolation yields $\sigma_d = -1304$ ppm. However, it was later demonstrated that many polyoxotungstates having WO_6 octahedra with C_{4v} symmetry do not exhibit this dependence. So the correlation between LCT and ^{183}W chemical shift is not a general observation.

Acerete et al. [18] reported the investigation of ^{183}W isotropic shifts for paramagnetic species, α-$[Co^{II}O_4W_{12}O_{36}]^{6-}$ and α-$[Co^{III}O_4W_{12}O_{36}]^{5-}$. The observed chemical shift δ_{obs} consists of two terms: diamagnetic shift δ_{dis} and isotropic shift δ_{iso}. The δ_{dis} is usually estimated as the above-mentioned chemical shifts for an isostructural diamagnetic species. δ_{iso} is made up by the contact term δ_{con} and the dipolar term δ_{dip}. The isotropic shift in the spectra of paramagnetic species arises from an electron–nuclei interaction via direct contact hyperfine coupling and/or a through-space dipolar mechanism. The Fermi-contact shift is a direct measure of the unpaired spin density delocalized onto the s orbital around the resonating nucleus and is taken as evidence of "metal–ligand" covalency. The dipolar contribution arises from through-space interaction between an electronic magnetic moment and the observed nucleus, and can be expanded to a non-hydrogen nucleus by subdividing the δ_{dip} into two terms: "ligand-centered" dipolar contribution, δ^L_{dip}, and "metal-centered" dipolar contribution, δ^M_{dip}, yielding:

$$\delta_{obs} = \delta_{dis} + \delta_{con} + \delta^L_{dip} + \delta^M_{dip} \quad (2)$$

where L represents W and M is the paramagnetic center Co^{II} or Co^{III}. The experimental and predicted chemical shifts are listed in Table 1.

The data in Table 1 show that: (i) the experimental data are consistent with the chemical shifts in the paramagnetic system being be treated as a sum of the individual components; (ii) for a paramagnetic system the isotropic shift is the most important contribution to the total shift, wherein the dipolar shift is obviously predominant; and (iii) for the system with a very regular central tetrahedron $Co^{II}O_4$, the δ^L_{dip} dominates the δ_{obs}, while for a system with a significantly Jahn–Teller distorted central tetrahedron $Co^{III}O_4$ the δ^M_{dip} shows the largest contribution to the total shift.

Table 1
Calculated and experimental chemical shifts of the paramagnetic POMs[a]

Anion	δ_{dis}	δ_{con}	δ^L_{dip}	δ^M_{dip}	δ_{obs}
α-$[Co^{II}O_4W_{12}O_{36}]^{6-}$	−109	−9.9 ± 12.6	−780 to −790	+13	−887.6
α-$[Co^{III}O_4W_{12}O_{36}]^{5-}$	−81	−24 ± 30	−690 to −580	−1300	−1993.7

[a] Calculated values: δ_{dis}, diamagnetic shift; δ_{con}, contact shift; δ^L_{dip}, "ligand-centered" dipolar contribution; δ^M_{dip}, "metal-centered" dipolar contribution; δ_{obs}, experimental value.

3.2. Coupling constants

The magnitude of the coupling constant is a measure of the spin–spin interaction between adjacent nuclei under consideration which can provide some structural information. Lefebvre et al. [19] observed the mononuclear coupling constant $^2J_{W–O–W}$ of POMs, $H_2W_{12}FO_{39}^{5-}$ and β-$H_4SiW_{12}O_{40}$, as 7% satellites to the main lines. They found that the magnitude of the coupling constant $^2J_{W–O–W}$ varied with W–O–W bond angle. Combined the single crystal analysis they suggested a general rule: a pair of tungsten atoms sharing a common oxygen atom (angle about 150°) has $^2J_{W–O–W}$ values of about 15–22 Hz, while those edge-sharing a pair of oxygen atoms (angle about 120°) have $^2J_{W–O–W}$ values in the 5–7 Hz range. Large $^2J_{W–O–W}$ values ∼30 Hz were found in Wells–Dawson structure anions (W–O–W bond angle about 160°) [20], i.e., $^2J_{W–O–W}$ depends on the oxygen bridging bond angle. The less bent bridging bond results in a greater interaction of the bridging oxygen orbital with the tungsten atoms and therefore the larger values of $^2J_{W–O–W}$. In complexes with metallic vacancies, very small corner coupling (<10 Hz) was observed for coupling tungsten atoms in the vicinity of the vacancy. This difference with respect to the saturated anions had been explained by the existence of a long W–O bond (210–220 pm), where the bridging oxygen atom was *trans* to a terminal one [21–23]. Thouvenot and co-workers [21,22] found larger variations in the $^2J_{W–O–W}$ values (37–4.9 Hz) for vertex sharing in $P_4W_{14}O_{58}^{12-}$, γ-$SiW_{10}O_{36}^{8-}$ and $NH_4As_4W_{40}O_{140}^{23-}$. The normal coupling constants are recovered by filling the lacuna [24,25]. Kazansky [26] noted a general trend of decreasing $^2J_{W–O–W}$ with increasing sum of the two W–O bond lengths ($R_1 + R_2$) in a bridging bond W–O–W, when he investigated the correlation between coupling constant and POM geometry. In addition, the relative intensity of the $^2J_{W–O–W}$ satellite yields evidence for the number of tungsten atoms coupled to the observed nuclei [26]. These results provide a rational basis for distinguishing the W–W atom mode of connectivity in the metal atom backbone.

3.3. ^{183}W NMR spectrum and structure of POMs

Hundreds of POM ^{183}W NMR spectra have been reported since the first ^{183}W NMR POM spectrum observed by Acerete et al. [6] in 1979. The chemical shifts of POMs with typical structure are listed in Table 2.

3.3.1. Keggin structure anions and their derivatives

A Keggin anion $XW_{12}O_{40}^{(8-n)-}$ (n is the charge of central atom, Fig. 1) with T_d symmetry has 12 tungsten atoms which are located in the same chemical and magnetic environment, and therefore exhibit a very sharp line with a half-peak width less than 1 Hz (Table 2) [6,17], except $PW_{12}O_{40}^{3-}$ whose line is split into a narrow doublet by coupling between ^{31}P and ^{183}W, $^2J_{P–O–W} \approx 1$ Hz. The chemical shifts vary with the central atom, showing the sensitivity of ^{183}W to the central atom. Isomerization of the Keggin anion occurs when one or two of the four triplets is rotated by 60° around its C_3 axis, forming the β- or γ-isomer, respectively. The symmetry of the $XW_{12}O_{40}^{(8-n)-}$ isomers decreases in the sequence of α-isomer (T_d) → β-isomer (C_{3v}) → γ-isomer (C_{2v}), the number of resonance lines increases in the same sequence [16,18,23]. Kazansky [26] investigated the correlation of chemical shift with the geometry of POMs and the W–O distances and bond angles. He noted with the reduction of the mean bond length (R) there is an increase in shielding constant of the atom considered, that is, the δ of the atom considered shifts upfield. For example the mean distance of the W–O–W bridge bond in $XW_{12}O_{40}^{(8-n)-}$ decreases in the sequence of P^V, Si^{IV}, $(2H)^{2+}$ and the chemical shifts move upfield in the same sequence (see Table 2). The δ values in the β-$SiW_{12}O_{40}^{4-}$ ^{183}W NMR spectrum shift upfield as the mean bond length of the W–O–W bridge bonds decreases [26]. The same tendency appears in the NMR spectra of Wells–Dawson anions. In γ-SiW_{12} (Fig. 2), two unique tungsten atoms (denoted as D) linked to each other by sharing an edge and with almost perfect coplanarity of the W $5d_{xy}$ orbitals are found to be quite shielded (−165 ppm). The other tungsten atoms give rise to three lines in the range of −100 to −127 ppm [24]. Decreasing the symmetry of the whole anion results in a decreased weight averaged chemical shift value despite the fact that the low-energy side of the first CT band in the UV spectrum being slightly red-shifted [26].

Removal of one WO^{4+} group from the Keggin anion produces a lacunary anion $XW_{11}O_{39}^{n-}$ in which the W atoms divided into six groups, five symmetric equivalent pairs of W atoms and a single structurally unique W atom, and therefore six lines occur in their ^{183}W NMR spectra with intensity ratio 2:2:1:2:2:2 (the order of lines may be vary for individual anion) [6,28,29,47]. The removal of one WO^{4+} group also results in a broadening of lines and a variety of $^2J_{W–O–W}$ values. Occupation of the vacancy in $XW_{11}O_{39}^{n-}$ by other metallic atoms, forming so-called mono-substituted anions $XMW_{11}O_{40}^{n-}$, does not change the symmetry of the anion (C_s) and the spectral envelope [17,45,48–55]. The resonance lines of 11-W species show a general upfield shift except for those W atoms located around the vacancy where the

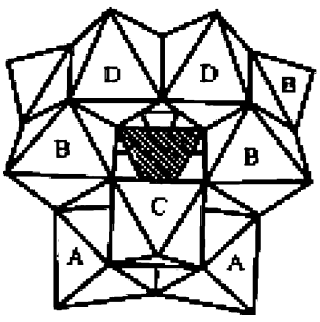

Fig. 2. Polyhedral representation of γ-$SiW_{12}O_{40}^{4-}$ anion.

Table 2
Chemical shifts of POMs with typical structures

Anion	Symmetry	Chemical shift (δ) in ppm (intensity ratio)[a]	References
$[\alpha\text{-}XW_{12}O_{40}]^{(8-n)-}$	T_d	−99.4 (P), −104 (Si), −131 (B), −96 (Zn), −887.6 (Co^{2+})[b], −113.0 ($(H_2)^{2+}$)[b]	[17,18]
$\beta\text{-}SiW_{12}O_{40}^{4-}$[c]	C_{3v}	−103.5, −104.0, −120.2 (1:2:1)	[19]
$\gamma\text{-}SiW_{12}O_{40}^{4-}$[d]	C_{2v}	−104.7, −116.8, −127.4, −160.1 (2:1:2:1)	[24]
$\alpha\text{-}SiW_{11}O_{39}^{8-}$	C_s	−100.9, −116.2, −121.3, −127.9, −143.2, −176.2 (2:2:2:1:2:2)	[6]
$\alpha\text{-}SiVW_{11}O_{40}^{5-}$	C_s	−104.8, −105.6, −107.4, −117.5, −129.5, −131.9	[27]
$[La(SiW_{11}O_{39})_2]^{13-}$	C_{2v}	−105.2, −117.4, −113.2, −136.6, −162.2, −169.5 (2:1:2:2:2:2)	[28]
$[La(PW_{11}O_{39})_2]^{11-}$	C_2	−144, −130, −150, −128, −104, −117 (2:2:2:2:2:1)	[29]
$A\text{-}\alpha\text{-}1,2\text{-}SiV_2W_{10}O_{40}^{6-}$	C_{2v}	−83.5, −86.0, −111.7, −122.7, −142.5 (2:2:3:2:1)	[27]
$A\text{-}\alpha\text{-}1,2,3\text{-}SiV_3W_9O_{40}^{7-}$	C_{3v}	−91.5, −136.7 (2:1)	[27]
$A\text{-}\beta\text{-}1,2,3\text{-}SiV_3W_9O_{40}^{7-}$	C_{3v}	−115.4, −120.0 (2:1)	[27]
$[(ZrOH)_3(\beta\text{-}SiW_9O_{34})_2]^{11-}$[e]	D_{3h}	−114.0, −189.0 (1:2)	[30]
$[Zn_4(H_2O)_2(PW_9O_{34})_2]^{10-}$	C_{2h}	−90.7, −102.5, −117.8, −130.5, −135.6 (1:2:2:2:2)	[31]
$\alpha\text{-}P_2W_{18}O_{62}^{6-}$[b]	D_{3h}	−128.1, −173.8 (1:2)	[32]
$\beta\text{-}P_2W_{18}O_{62}^{6-}$[b]	C_{3v}	−111.6, −131.1, −171.1, −191.2 (1:1:2:2)	[32]
$\gamma\text{-}As_2W_{18}O_{62}^{6-}$	D_{3h}	−110.0, −166.0 (1:2)	[33]
$H_4PW_{18}O_{62}^{7-}$		−127.8, −135.7, −144.9, −181.3 (2:1:1:2)	[34]
$H_6W_{18}O_{62}^{10-}$[f]	C_{2v}	−122.0, −146.6, −161.1 (1:1:1)	[35]
$\alpha_2\text{-}P_2W_{17}O_{61}^{10-}$[b]	C_s	−127.8, −140.8, −159.6, −175.6, −179.6, −218.9, −222.7, −225.0, −242.3 (2:2:2:2:1:2:2:2:2)	[17]
$\alpha_1\text{-}P_2W_{17}O_{61}^{10-}$	C_1	−200.1, −203.7, −210.3, −241.3, −214.6, −225.5	[36]
$\alpha_2\text{-}P_2NbW_{17}O_{62}^{7-}$	C_s	−108.1, −129.2, −141.9, −172.5, −176.1, −178.9, −181.3, −185.2, −189.5 (2:2:1:2:2:2:2:2:2)	[37]
$\alpha_1\text{-}P_2Zn(H_2O)W_{17}O_{61}^{8-}$	C_s	−99.4, −117.4, −123.0, −151.9, −157.7, −167.6, −174.2, −175.7, −177.3, −193.3, −200.1, −203.7, −210.3, −214.1, −214.6, −225.5	[38]
$[La(\alpha_2\text{-}P_2W_{17}O_{61})_2]^{17-}$	C_2	−137.6, −146.8, −179.0, −180.5, −193.8, −194.1, −213.7, −218.5, −219.6, −239.5 (2:2:2:1:2:2:2:2:2:2)	[28]
$\alpha\text{-}As_2Mo_2W_{16}O_{62}^{6-}$	C_s	−114.1, −124.9, −126.6, −145.3, −146.6, −147.6, −147.8, −151.4, −155.0 (1:1:2:2:2:2:2:2:2)	[39]
$[Ce_4(OH)_2(H_2O)_9(P_2W_{16}O_{59})_2]^{14-}$	C_s	−295.5, −90.3, +44.1, +121.1, +123.2, +173.5, +186.7, +188.4	[40]
$\alpha\text{-}1,2,3\text{-}P_2V_3W_{15}O_{62}^{9-}$	C_{3v}	−157.3, −180.6, −228.5 (1:2:2)	[41]
$[Zn_4(H_2O)_2(P_2W_{15}O_{56})_2]^{16-}$	C_{2h}	−150.4, −160.5, −162.0, −180.0, −238.2, −143.4, −244.7 (1:2:2:2:2:2:2:2:2)	[42]
$\alpha\text{-}P_2Mo_6W_{12}O_{62}^{6-}$	C_{2v}	−130.3, −166.6, −179.9 (4:4:4)	[33]
$\alpha\text{-}P_2(NbO_2)_6W_{12}O_{56}^{12-}$	C_{2v}	−122.4, −158.1, −203.5 (4:4:4)	[43]
$TeW_6O_{24}^{6-}$	D_{6h}	−115.8	[44]
$W_7O_{24}^{6-}$[b]	C_{2v}	+269.2, −98.8, −178.9 (1:4:2)	[13]
$H_2W_{12}O_{42}^{10-}$	C_2	−108.2, −110, −114.5, −141.4 (1:2:1:2)	[13]
$W_6O_{19}^{2-}$[c]	O_h	+58.9	[45]
$VW_5O_{19}^{3-}$[e]	C_{4v}	+76.4, +75.9 (4:1)	[27]
$V_2W_4O_{19}^{4-}$	D_{4h}	+70.3, +69.4 (2:2)	[27]
$W_{10}O_{32}^{4-}$[b]	D_{4h}	−37, −173 (4:1)	[46]
$[La(W_5O_{18})_2]^{9-}$[b]	D_{4h}	+31.0, −13.4 (4:1)	[28]
$NaP_5W_{30}O_{110}^{14-}$	C_{5v}	−287.8, −275.5, −209.7, 207.6 (1:1:2:2)	[33]

[a] Counterion is Li^+ in D_2O except those labeled by footnotes b–f.
[b] Na^+ in D_2O.
[c] $(C_4H_9)_4N^+$ in $(CH_3)_2NCHO$(DMF).
[d] $(C_4H_9)_4N^+$ in DMSO.
[e] $(C_4H_9)_4N^+$ in CH_3CN.
[f] *n*-Pr_4N^+ in propylene carbonate.

increased electronic anisotropy produces a downfield shift. Thus, the center of gravity of the ^{183}W NMR spectrum remains relatively constant for a given heteroatom, and the relative distribution of lines is much the same for a homologous series, producing a remarkable similarity in the qualitative appearance of the spectra [27].

The monovacant anion $XW_{11}O_{39}^{n-}$ can act as four-dentate ligand and forms a series of complexes, $Ln(XW_{11}O_{39})_2^{n-}$ (Ln represents lanthanides) [56] or $Ce(XW_{11}O_{39})^{n-}$ [57], in which lanthanide ions lie in a square-antiprismatic coordination geometry. The NMR data (six lines) for the $Ln(PW_{11}O_{39})_2^{n-}$ family of compounds show a symmetrical

structure (C_{2v}) for the early lanthanides and after gadolinium the data (more than nine resonance lines) are consistent with rotation of one $PW_{11}O_{39}$ relative to the other and inequivalence of the tungsten atoms of each heteropolytungstate [28,29,55].

Removal of three W atoms from $XW_{12}O_{40}^{n-}$ produces three lacunary anions $XW_9O_{34}^{m-}$ [7]. If the three removed W atoms come from one triplet (W1, W4, W9 in Fig. 1), a B isomer is obtained; and if they come from three triplets (W1–W3), an A isomer is formed. In both A and B isomers the W atoms are divided into two groups: one group comprises a six-atom belt and the other group three polar atoms, a triplet in A isomer or a triad in B isomer. The A and B isomers have same C_{3v} symmetry and should theoretically give a two-line spectrum. However, there has been no direct observation of these two anionic spectra due to their low solubility and instability in aqueous solution. Very recently, Errington et al. [58] reported the synthesis and ^{183}W NMR spectrum of a brominated polyoxotungstate A-$PW_9O_{26}Br_6^{3-}$. It does exhibit two lines with $^2J_{W-O-W} = 25$ Hz, showing an A-type of tri-vacant anion. Three vacant sites can be occupied by other metal atoms, resulting in the so-called three-substituted anion, $XM_3W_9O_{40}^{n-}$. The tri-lacunary anion and the tri-substituted anion, $XW_9O_{34}^{n-}$ and $XM_3W_9O_{40}^{n-}$, have the same symmetry (C_{3v}) and similar two-line NMR spectra [20,25,28,59–66] except in the cases with different kinds of M atoms [25] or protonation of the bridge oxygen atom [41]. There are also dimeric anions [(α-, β-$XM_3W_9O_{37}$)$_2$ (μ-O)$_3$]$^{n-}$ (X = Si, M = Ti, Nb; X = Ge, M = Ti) which also give two-line spectra [67–69].

When the $XW_9O_{34}^{n-}$ acts as a ligand two types of complex can be formed: Keggin sandwich anions M_3(α-, β-XW_9O_{34})$_2$ (M = Zr, Ce^{III}, Co, Cu, Pd, Sn) with C_{3h} symmetry and M_4(B-XW_9O_{34})$_2$ (X = P, As; M = Mn, Fe, Co, Ni, Cu, Zn) with C_{2h} symmetry. The former retains the two-line spectrum [30,70–73] and the latter has a four line spectrum [31,74,75]. A- and B-$XW_9O_{34}^{n-}$ anions have two isomers, α and β [7]. Two isomers of the A-$XW_9O_{34}^{n-}$ have the same symmetry and the same two-line spectrum, but the difference of the two chemical shifts $\Delta\delta$ are not identical, in general $\Delta\delta(\alpha) > \Delta\delta(\beta)$ for A-$XW_9O_{34}^{n-}$ and A-$XM_3W_9O_{40}^{n-}$, which can be used in distinguishing two isomers [63,64].

3.3.2. Wells–Dawson structure anions and their derivatives

An anion $X_2W_{18}O_{62}^{6-}$ (X = P, As) with the so-called Wells–Dawson structure also has α, β, γ isomers [7]. The α-isomer is constructed from two A-α-$XW_9O_{34}^{9-}$ via sharing the corner oxygen atoms of the six-atom belts, and has D_{3h} symmetry (Fig. 3) and a two-line spectrum [32]. A β-isomer is formed by rotating one polar triplet around the C_3 symmetry axis, it has C_{3v} symmetry, and has a four-line spectrum [32], the γ-isomer results from rotating two polar triplets around the C_3 symmetry axis and has the same symmetry and the same two-line spectrum as the α-isomer does [33]. Mono-lacunary and mono-substituted derivatives $X_2W_{17}O_{61}^{n-}$ and $X_2MW_{17}O_{62}^{m-}$ have two

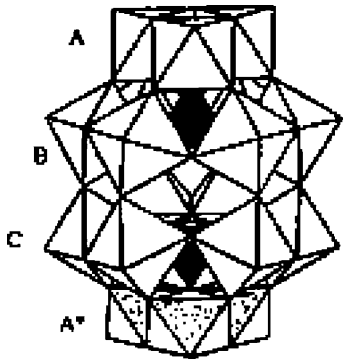

Fig. 3. Polyhedral representation of Wells–Dawson anion.

isomers: α_1-isomer (one W atom removal from six-atom belt) and α_2-somer (one W atom removal from polar triplet). Mono-lacunary [17,36] and mono-substituted derivatives including complexes $X_2MW_{17}O_{62}^{n-}$ [37,38,76] and $Ln(X_2W_{17}O_{61})_2^{n-}$ [29,77–79] of one isomer have the same spectral envelope. Like the Keggin anion, the Wells–Dawson anion also yields the tri-lacunary anion and tri-substituted complexes which give three line spectra [33,41,76,80–83], as well as sandwich complexes [42,84].

In the six-substituted $P_2Mo_6W_{12}O_{62}^{6-}$ anion one each of the polar Mo atom is in each triplet and two Mo atoms are in each belt. The two polar Mo atoms are connected to their nearest neighbor tungsten atom by edge-sharing while the four belt Mo atoms are linked to their nearest neighbors by corner sharing. It is this structure that gives the three tungsten NMR lines in the ratio of 4:4:4 [33,43].

3.3.3. Lindqvist anion and its derivatives

$W_6O_{19}^{2-}$ is called Lindqvist anion in which six W atoms lie in identical environments (Fig. 4). It has O_h symmetry and gives a one-line spectrum [45,51] with the largest chemical shift for anions having MO_6 C_{4v} symmetry. Its derivatives $W_{10}O_{32}^{4-}$ are built up by two corner-shared $W_5O_{18}^{6-}$ formed by removing WO^{4+} group from $W_6O_{19}^{2-}$. As in the case of α-$X_2W_{18}O_{62}^{6-}$, the $W_{10}O_{32}^{4-}$ has polar W atoms (2W) and belt W atoms (8W) and therefore has a two-line spectrum [12,46,81,85]. Another kind of derivative, $XW_{10}O_{36}^{n-}$ or $X(W_5O_{18})_2^{n-}$ where X is a lanthanide or actinide, consists of one central X atom and two $W_5O_{18}^{6-}$

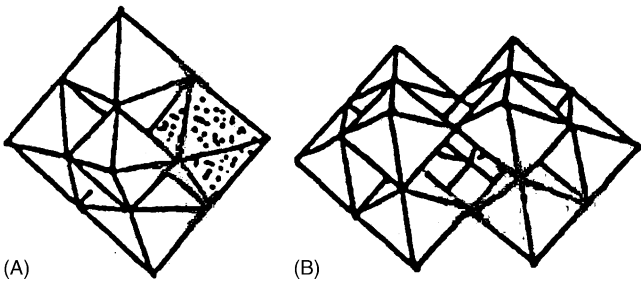

Fig. 4. Polyhedral representations of Lindqvist anion (A) and its derivative (B).

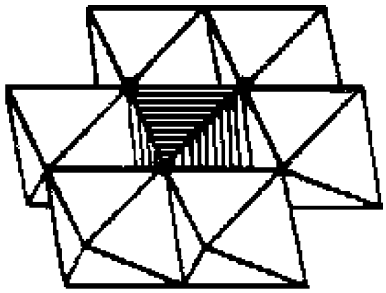

Fig. 5. Polyhedral representation of Anderson anion.

ligands and they have the same symmetry (D_{4h}) and same spectral envelope [27,83,86,87] as does $W_{10}O_{32}^{4-}$. The W atoms in $W_6O_{19}^{2-}$ can also be substituted by other metal atoms, forming mono- and bi-substituted derivatives, such as $W_5O_{19}\{Mo(NO)\}^{3-}$ and $MW_5O_{19}^{3-}$, $M_2W_4O_{19}^{4-}$ (M = V^V, Nb^V) whose spectra contain two lines [28,88,89,90] with intensity ratio of 4:1 for the first two species and 2:2 for the last one. The substitution of organic group for the oxygen atom of $Nb_2W_4O_{19}^{4-}$ results in a three line spectrum [90].

3.3.4. Anderson anion

$TeW_6O_{24}^{2-}$ (Fig. 5) is built up of a central atom M^{m+} with an octahedral configuration and six edge shared WO_6 octahedra forming a ring around the M^{m+}, very similar to $MMo_6O_{24}^{n-}$ [7]. Each WO_6 octahedron is distorted to C_{2v} symmetry with two *cis*-terminal oxygens. All the W atoms lie in the same environment and the anion gives only one line in its ^{183}W NMR spectrum [44].

3.3.5. Isopolytungstate anions $H_2W_{12}O_{42}^{10-}$ and $W_7O_{24}^{6-}$ [13]

Isopolytungstate anions $H_2W_{12}O_{42}^{10-}$ and $W_7O_{24}^{6-}$ are the products of acidifying WO_4^{2-} solution. At room temperature $W_7O_{24}^{6-}$ easily transforms to $H_2W_{12}O_{42}^{10-}$ (after several hours), at elevated temperature this transformation is incomplete and occurs more slowly. Aging the $W_7O_{24}^{6-}$ concentrated solution leads to crystallization of $Na_{10}H_2W_{12}O_{42}{\cdot}27H_2O$. In the presence of Li^+, the $H_2W_{12}O_{42}^{10-}$ remains in the solution. $H_2W_{12}O_{42}^{10-}$ has a complex structure with four structural types of WO_6 octahedra (Fig. 6A) and its ^{183}W NMR spectrum show four resonance signals with an intensity ratio 1:2:1:2, which corresponds to the anion structure in the crystalline state. Upon heating the solution, the $H_2W_{12}O_{42}^{10-}$ anions partly

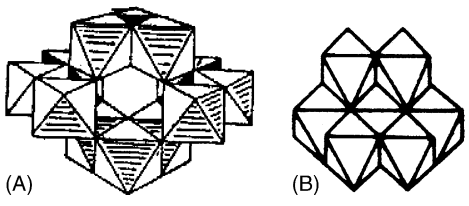

Fig. 6. Polyhedral representation of $H_2W_{12}O_{42}^{10-}$ (A) and $W_7O_{24}^{6-}$ (B).

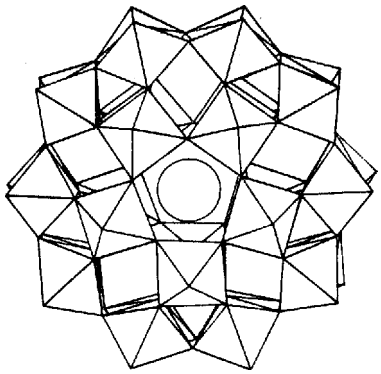

Fig. 7. Polyhedral representation of $NaP_5W_{30}O_{110}^{15-}$ [93] showing WO_6 octahedra and the central Na (opened circle).

transform to $W_7O_{24}^{6-}$. The $W_7O_{24}^{6-}$ with a same structure as $Mo_7O_{24}^{6-}$ has three structural types of tungsten atoms (Fig. 6B) and therefore produces three lines in a wide range (+269 to −179) with an intensity ratio 1:4:2 in its ^{183}W NMR spectrum.

3.3.6. Cryptate anions

A large anion $NaP_5W_{30}O_{110}^{15-}$ (Fig. 7) is built up of five fragments (PW_6) of the Keggin structure by vertex sharing, being called a cryptate anion. The interior sodium disturbs the original D_{5h} symmetry because it is located in one of the two pentagonal planes formed by the O_a atoms which are shared by the P atoms and the W atoms in the five-membered rings of the WO_6 octahedra. The non-equivalent upper and lower parts of the anion result in a four line ^{183}W NMR spectrum [33,91,92]. The sodium cation may be replaced by larger Bi^{III}, Ca^{II}, U^{IV} and some lanthanide ions. The replacement of the larger cation for Na^+ ion does not change the anionic symmetry from C_{5v} to D_{5h} and does not change the spectral envelope [91].

Another cryptate anion $[(B\text{-}\alpha\text{-}AsW_9O_{34})_4(WO_2)_4]^{28-}$ (denoted as As_4W_{40}, Fig. 8) can be viewed as a derivative of $AsW_9O_{34}^{9-}$, in which four $AsW_9O_{34}^{9-}$ units are linked by additional tungsten atoms. The W atoms in $[(B\text{-}\alpha\text{-}AsW_9O_{34})_4(WO_2)_4]^{28-}$ are divided into six groups and give six signals with intensity ratio 2:2:1:2:2:1 [94]. This anion has the ability to accommodate alkali, alkaline earth, and lanthanide cations in the central cryptate site (S1) as well as di- or tri-valence 3d metal cations and Ag^+ in four lacunary sites (S2) [95–97].

Wasssermann and Pope [98] reported the crystal structure analysis of $Na_{40}\{[(H_2O)_{10}Ln^{III}(Ln_2OH)(B\text{-}\alpha\text{-}AsW_9O_{34})_4(WO_2)_4]_2\}{\cdot}nH_2O$ (abbreviated as $Ln_3As_4W_{40}$) (Ln = Ce, Sm, Gd) and $Na_{16}\{[Ba(H_2O)_{10}(Ce^{III}{}_2OH)_2(B\text{-}\alpha\text{-}AsW_9O_{30})_4(WO_2)_4]_n\}{\cdot}51H_2O$. The single crystal structural analysis of $Ln_3As_4W_{40}$ revealed the site of Ln, one in S3 and two in S2 (Fig. 8). There is a linkage between adjacent Ln units, via two W–O–Ln bonds arranged in pairs $(Ln_3As_4W_{40})_2$, and assuming overall C_i symmetry; 40 resonance lines are expected. However, 9 lines were observed,

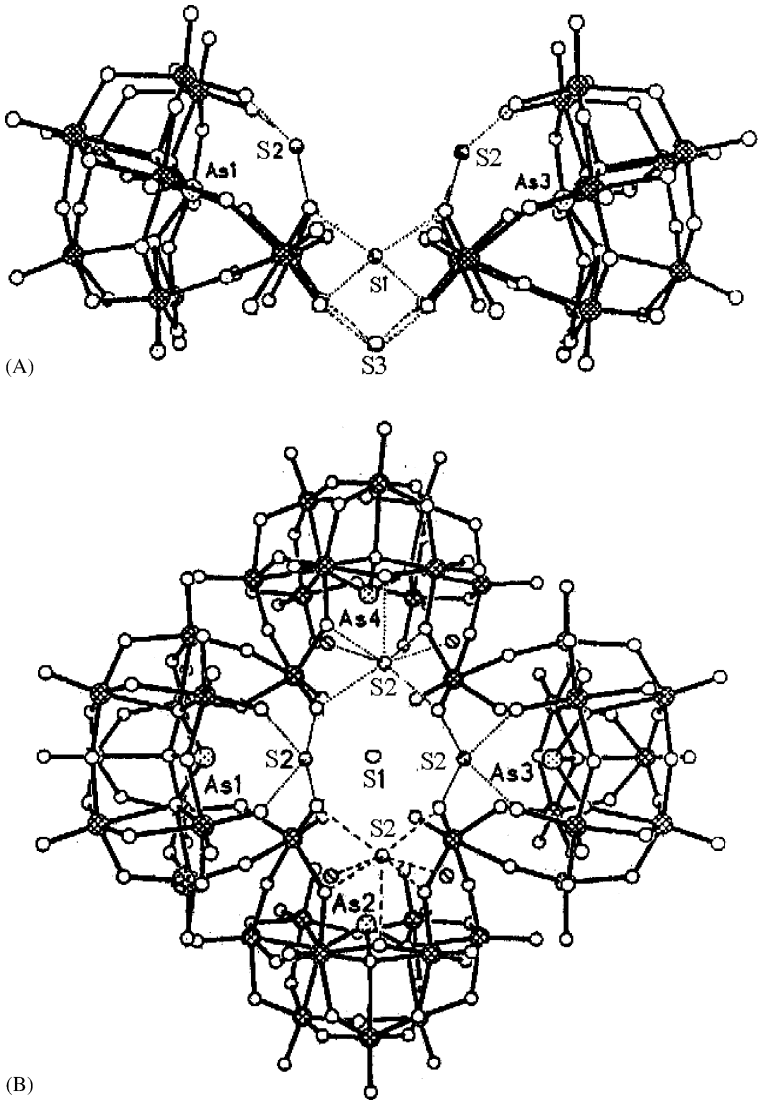

Fig. 8. Cryptate anion $[(B\text{-}\alpha\text{-}AsW_9O_{34})_4(WO_2)_4]^{28-}$ showing the S1, S2, S3 sites.

between −50 and −250 ppm, for the Ce and Nd complexes, which approaches that of the expected monomeric unit with D_{2d} symmetry which should exhibit 11 lines, 9 of intensity 2 and 2 of intensity 1. Thus, $Ln_3As_4W_{40}$ is dimeric in the solid state, and in solution it is monomeric due to the hydrolysis of W–O–Ln bonds. In the same way, as the ^{183}W NMR experiments showed, $Ln_4As_4W_{40}$ (Ln all in S2 sites) in solution is monomeric and gives a simple NMR spectrum corresponding to anion of D_{2d} symmetry. However, the resonance signal for the bridging tungsten atom between the AsW_9 units could not be detected (Ln = La; −110.7(2), −115.5(2), −153.1(2), −194.5(2)).

A new polyanion $[(UO_2)_3(H_2O)_6(AsW_9O_{34})_3(WO)_3]^{15-}$ [99] is built up by three AsW_9 units which were linked by both U atoms and W atoms. Its six-line spectrum in solution indicated a structure with C_{3v} symmetry, or with one of virtual C_{3v} symmetry as a result of rapid interconversion among the three arrangements (−78.3, −92.7, −98.8, −106.4, −151.2 and −206.0 ppm with an intensity ratio 2:1:2:2:2:1).

Another group of polyanions containing uranium $[M_2(UO_2)_2(PW_9)_2]^{12-}$ (M = K^+, NH_4^+, Na^+) was reported by Kim and Pope [100]. In the anions with M = K^+, NH_4^+, two A-$PW_9O_{34}^{9-}$ asymmetrically sandwich two uranyl cations forming a central crypt which is occupied by K^+ or NH_4^+ ion, another M ion may be considered as an external ion. These polyanions exhibited nine-line spectra with an approximate intensity ratio of 2:1:2:4:2:2:1:2:2, consistent with virtual C_s symmetry.

3.4. Paramagnetic species

3.4.1. Species with transition metal atoms

Paramagnetic polyoxometalates are formed when one or more transition metal atoms with unpaired electrons act as constituent of POMs either in the central site or in the

ligand site. The presence of the paramagnetic ions causes a great variation in the chemical shifts. In the case of a central paramagnetic ion, such as $CoW_{12}O_{40}^{5-/6-}$, 12 tungsten atoms are still in an identical environment and give a single line but with a remarkable upfield shift due to the delocalization of the unpaired electron over the whole anion [18]. The paramagnetic ion present in the ligand site of $XW_{11}MO_{40}H_2^{n-}$ (M = Fe^{III}, Mn^{II}, Cr^{III}, Ru^{III}, Co^{II}, Ni^{II}) [38,55,98,101,102,103] makes the resonance lines shift either up or low field and broaden, even disappear as shown in Table 3. The resonance signals which disappeared and those with large line width were assigned to those tungsten atoms nearest to the paramagnetic ion according to the unambiguous assignment of the lines in the Zn-analogue using the J_{w-O-w} connectivity pattern [38]. In these anions the W atom with intensity 1 is the most shielded.

Jorris et al. [38] found a marked difference in the ^{183}W shifts for $SiW_{11}MO_{40}H_2^{6-}$ and $PW_{11}MO_{40}H_2^{5-}$ (M = Ni^{2+}, Co^{2+}). The smaller shift for the former is consistent with the lower degree of spin delocalization deduced from the analysis of the EPR spectra of the corresponding reduced forms.

When POM contains two or more paramagnetic cations, the behavior of the NMR lines is not predictable. For example for A-$SiW_9Co_3O_{40}^{10-}$ where three Co^{II} atoms make up a three corner-shared triad, two ^{183}W lines, one with a large downfield shift (+708 ppm) and the other with an upfield shift (−690 ppm), are observed and assigned, respectively, to tungstens non-bonded and bonded to Co^{II} which broadens the resonance of the latter [61].

There are other paramagnetic systems involving lanthanides and actinides which are fairly fixed in some anions as heteroatoms (X): $XO_8W_{10}O_{28}^{n-}$, $X(PW_{11}O_{39})_2^{n-}$, $X(P_2W_{17}O_{61})_2^{n-}$, $XP_5W_{30}O_{110}^{n-}$. Fedotov et al. [86,88] recorded the NMR spectra of the $XO_8W_{10}O_{28}^{n-}$ system. These complexes have the same spectral envelope but the shifts caused by the paramagnetic lanthanides vary remarkably (Table 3). The ^{183}W shifts of $UW_{10}O_{36}^{8-}$ are much larger than that observed for $PrW_{10}O_{36}^{9-}$, an electronic analog of the U complex, showing a greater participation of the U 5f orbital in electron transfer into the W 5d orbital [104].

The ^{183}W NMR spectrum of $[\{Ce(H_2O)_2(\alpha_1\text{-}P_2W_{17}O_{61})\}_2]^{14-}$ [77] consisted of 17 lines of similar intensity, consistent with the C_1 symmetry of α_1-isomer. Thirteen lines appeared between −110 and −215 ppm, the other four were observed between +100 and +340 ppm and were assigned to the W atoms adjacent to the paramagnetic Ce atoms.

The Eu atom in $EuP_5W_{30}O_{110}^{11-}$ formed by replacement of Eu for the sodium cation in $NaP_5W_{30}O_{110}^{14-}$ modified the symmetry of the anion to be C_{5v} rather than the original D_{5h} symmetry of $P_5W_{30}O_{110}$ as shown by its ^{183}W NMR spectrum which had the same pattern as that of $NaP_5W_{30}O_{110}^{14-}$. The replacement of Eu^{3+} for Na^+ and the occupation of Eu^{3+} in a similar site in the complex were confirmed by a significant displacement of one of 5W lines to a different frequency [91].

The missing resonances for two W atoms in $BaCe_4As_4W_{40}$ and $KCe_4As_4W_{40}$ are presumed to be a consequence of several neighboring paramagnetic (Ce) ions [98].

3.4.2. Reduced species

POMs may be reduced reversibly by one or more electrons producing intensely colored species—'heteropoly blues' [7]. Retention of the original structure upon reduction is due to the added electron occupying a non-degenerate d_{xy} orbital which leaves all the bonding orbitals unchanged. The bridging oxygen atoms provide pathways for electron delocalization. The heteropoly blues with odd electrons are paramagnetic and those with an even number of electrons are generally diamagnetic [12,24,93,105–107]. Table 4 gives chemical shifts of some two-electron reduced POMs.

A single ^{183}W NMR line in the reduced $SiW_{12}O_{40}^{6-}$ (2e) [105,108] which is deshielded relative to the oxidized parent by 60 ppm [105] indicates the equivalence of all W atoms with a delocalized electron pair (bipolaron) [104].

Table 3
Chemical shifts of paramagnetic POMs

Anion	Symmetry	Chemical shift (δ) in ppm (intensity ratio)	References
$Co^{II}W_{12}O_{40}^{6-}$	T_d	−887.6	[18]
$Co^{III}W_{12}O_{40}^{5-}$	T_d	−1993.7	[18]
$SiW_{11}Co(D_2O)O_{39}^{6-}$	C_s	+437.6, +390.2, −222.2, −280.2 (2:2:2:1)[a]	[38]
$SiW_{11}Ni(D_2O)O_{39}^{6-}$	C_s	+328, +308, −134, −225[a]	[38]
$PW_{11}Ru^{III}(H_2O)O_{39}^{4-}$	C_s	−111.5, −146.3, −199.5 −559.5 (2:2:2:1)[a]	[101]
$PW_{11}Co(D_2O)O_{39}^{5-}$	C_s	+818, +725, −192, −256 (2:2:2:1)[a]	[38]
A-$SiW_9Co_3(H_2O)_3O_{37}^{10-}$	C_{3v}	+708, −690 (1:2)	[61]
α_2-$P_2Co(D_2O)W_{17}O_{62}^{10-}$	C_s	+534, +476, −143, −153, −200, −232, −236 (2:2:3:2:4)[a]	[27]
$EuW_{10}O_{36}^{9-}$	D_{4h}	−18, −611 (4:1)	[86,87]
$CeW_{10}O_{36}^{9-}$	D_{4h}	+155, +51	[86,87]
$PrW_{10}O_{36}^{9-}$	D_{4h}	+387, +53	[86,87]
$EuP_5W_{30}O_{110}^{12-}$	C_{5h}	+62.5, −201.7, −209.5, −297.5 (1:2:2:1)	[91]
$BaCe_4As_4W_{40}O_{130}H_2^{16-}$	D_{2d}	+106.1, +115.5, +191.3, +196.6 (2:2:2:1)[a]	[98]
$KCe_4As_4W_{40}O_{130}H_2^{17-}$	D_{2d}	+104.9, +114.1, +183.2, +194.3 (2:2:2:1)[a]	[98]

[a] Some lines were not observed.

Table 4
Chemical shifts of some two-electron reduced POMs

Anion	Chemical shift (δ) in ppm (intensity ratio)	References
α-$SiW_{12}O_{40}^{6-}$	−43	[108]
γ-$SiW_{12}O_{40}^{6-}$	489, −63, −124, −131 (2:2:1:1)	[24]
γ-$SiW_{12}S_2O_{38}^{6-}$	1041, −121.3, −144.6, −184.4 (1:2:2:1)	[93]
γ-$SiMo_2S_2W_{12}O_{38}^{6-}$	−122.9, −145.4, −177.0 (2:2:1)	[93]
$CoW_{12}O_{40}^{8-}$	−549	[105,106]
$P_2W_{18}O_{62}^{8-}$	−298, −49.8 (1:2)	[108]
α_1-$P_2W_{17}MoO_{62}^{8-}$	414, 62, −22, −123, −124, −128, −175, −192 (2×), −204, −206, −209, −220, −233, −254, −309	[107]
α_2-$P_2W_{17}MoO_{62}^{8-}$	210, −191, −59, −111, −180, −202, −235 (2:1:8:2:2:2)	[107]
α-$P_2W_{15}Mo_3O_{62}^{8-}$	−149, −226, −238 (1:2:2)	[108]
α-$P_2W_{12}Mo_6O_{62}^{8-}$	−149, −191, −171 (4:4:4)	[107]
$W_{10}O_{32}^{6-}$	300, −14 (4:1)	[12]

In contrast, the electrons in reduced γ-$SiW_{12}O_{40}^{6-}$ cause a large shift at +489 and −63 ppm to the two ^{183}W lines with intensity four due to delocalization of the electrons over the eight equivalent adjacent tungstens ($W_{2B}W_{2A}W_{2A}W_{2B}$), the other lines undergo small shifts indicating small partial delocalization of electrons onto the four separately located tungsten atoms (C and D sites in Fig. 2) [24]. Comparison of the spectra of γ-$SiW_{12}S_2O_{38}^{6-}$ and γ-$SiMo_2S_2W_{12}O_{38}^{6-}$ makes it clear that the line at +1041.2 ppm may be assigned to the W atoms (D sites) in a sulfur environment and the added two paired electrons are delocalized thereon [93].

Decatungstate $W_{10}O_{32}^{6-}$ has two distinct types of tungsten atoms in two square arrays and in two apical sites. After reduction the paired electrons are delocalized over eight adjacent tungsten atoms bound by linear bridges W–O–W and cause a large downfield shift in the resonance line of 8 W [12].

Reduced species with a Wells–Dawson structure exhibited various changes in chemical shifts. The large down field shift, from −173.8 ppm (oxidized anion) to −49.8 ppm (reduced anion), of the two belts consisting of 12 octahedra of reduced anion $P_2W_{18}O_{62}^{8-}$ is taken as evidence for the delocalization of the bipolaron on these atoms; and the large upfield shift of the six polar atoms from –128.1 ppm (oxidized anion) to −172 ppm (reduced anion) is taken as normal shielding for the reduced systems [108]. In the reduced anion $P_2Mo_3W_{15}O_{62}^{8-}$ the shifting was relatively smaller with respect to that of $P_2W_{18}O_{62}^{8-}$, but the addition of two electrons made the two lines of the belt W atoms separate remarkably (see Tables 4 and 5). It was supposed that the electron pair delocalized over three Mo atoms. It will be noticed that the signal of the W atoms closest to Mo atom, W_C, shifted the most and those furthest, W_A, the least (Fig. 3). Kozik et al. [107] have claimed that the electrons are evenly distributed over the six Mo atoms in the reduced anion $P_2Mo_6W_{12}O_{62}^{8-}$. None of the shifts exceeds −30 ppm and the smallest shift is assumed to occur on the four belt atoms furthest from the Mo atoms, in the spectrum of $P_2Mo_6W_{12}O_{62}^{8-}$ [108].

The α_2-$P_2MoW_{17}O_{62}^{8-}$ anion gives rise to nine lines due to the mirror plane in both the oxidized and reduced states [107], with δ values from +210 to −235 ppm in the reduced state (Table 4). For the α_1-isomer in which the Mo replaces a tungsten atom in the belt, all tungsten atoms are different and would display 17 different lines if they could be resolved. The introduction of two electrons results in a wide range of chemical shifts of 17 lines between +413 and −309 ppm [107]. In the analysis of the shifts in both cases, it was assumed [33,107] that one electron resided on the Mo atom and the second electron was delocalized over the six-membered belts.

The NMR spectrum of reduced species with paramagnetic center was recorded only for $Co^{2+}W_{12}O_{40}^{8-}$ (2e) [105,106]. The introduction of two electrons deshields the tungstens $\Delta\delta = +338$ ppm, a magnitude much larger than the observed $\Delta\delta = +51$ ppm for the diamagnetic $SiW_{12}O_{40}^{6-}$ (2e). This was explained [109] by a change in the delocalization mechanism of the unpaired electron spin density from Co(II) into the W orbitals.

Table 5
Chemical shifts of substituted POMs

Anion	Symmetry	Chemical shift (δ) in ppm (intensity ratio)	Reference
α-$P_2W_{18}O_{62}^{6-}$	D_{3h}	−128.1, −173.8 (1:2)	[32]
α-1,2,3-$P_2Mo_3W_{15}O_{62}^{6-}$	C_{3v}	−134, −180, −179 (1:2:2)	[108]
α-1,2,3-$P_2V_3W_{15}O_{62}^{9-}$	C_{3v}	−157.3, −180.6, −228.5 (1:2:2)	[76]
α-1,2,3-$P_2Nb_3W_{15}O_{62}^{9-}$	C_{3v}	−139, −209, −169 (1:2:2)	[82]
α_2-$P_2MoW_{17}O_{62}^{6-}$	C_s	−124, −129, −130, −170, −173, −175, −176, −178 (2:2:1:2:2:2:2:2)[a]	[76]
α_2-$P_2VW_{17}O_{62}^{7-}$	C_s	−105, −123, −165, −164, −177, −182, −184, −185, −209 (2:2:1:2:2:2:2:2:2)[a]	[76]

[a] Some lines were not observed.

The influence of subtle changes in the dimensions of the anion induced by a central atom will result in marked changes in the ^{183}W NMR shifts for the reduced species $XW_{12}O_{40}^{n-}$ with six electrons [110]. In the case of six electrons (six electrons on tungsten) an electronic isomerization takes place with the electrons localized in three W^{IV} $4d^2$ centers. This was proven by the large ^{183}W NMR shifts which exhibit $^2J_{W–W}$ coupling of the magnitude expected for a metal–metal bond [111]. Analysis of the spin–spin coupling $^2J_{W–O–W}$ shows that the six electrons are located in the triplet of edge shared octahedra.

3.5. Influence of other factors on chemical shifts

3.5.1. Charge and size of the substituted elements

The similarity of Mo to W results in two partially resolved lines at −179 and −180 ppm and small upfield shift (Table 5) in the ^{183}W NMR spectrum of $P_2Mo_3W_{15}O_{62}^{6-}$ assigned to the B(C) tungsten atoms in (Fig. 3) [108]. Edlund et al. [82] have shown that in $P_2Nb_3W_{15}O_{62}^{9-}$, where the W_3 triplet is replaced by Nb_3 whose size is bigger than Mo(VI) and the charge is smaller than Mo(VI), the B and C lines are separated with B shifted to −209 ppm even though the W_B atoms are separated by four bonds from the Nb atoms [82]. Similar shifts were observed for $P_2V_3W_{15}O_{62}^{9-}$ [76]. Two vanadium atoms sharing an edge (D sites) in γ-$SiV_2W_{10}O_{40}^{6-}$ induce high-field shifts for three ^{183}W NMR lines despite the edge-sharing that should give rise to deshielding of the nearby tungsten [24]. These all show the influence of size and charge of a substituent on the ^{183}W NMR chemical shifts.

The charge of the guest cation may markedly increase the shift range. For example in the case of the α$_2$-$P_2VW_{17}O_{62}^{7-}$, an electronic analog of α$_2$-$P_2Mo^{V}W_{17}O_{62}^{7-}$, which lacks a d^1 electron on the vanadium, the resonance lines are spread over the interval from −105 to −209 ppm [76]. The resonance line assigned to the unique tungsten in the triplet group which is related to the V^V by a mirror plane is observed at −165 ppm giving a −35 ppm shift from the anion α$_2$-$P_2MoW_{17}O_{62}^{6-}$ [76].

The presence of the six electrons in the t_{2g} orbitals of Ru^{II} in $PRuW_{11}O_{39}(H_2O)^{4-}$ results in a positive shift for practically all of the ^{183}W resonances [102]. Naturally, the largest shifts are expected to be for the W atoms closest to the Ru^{II} ion.

3.5.2. Replacement of terminal oxygen by halogen

Errington et al. [58] reported the ^{183}W NMR spectrum of a brominated polyoxotungstate anion $PW_9Br_6O_{26}^{3-}$ at $\delta = 189.1$ ppm, characteristic of the low-field chemical shift of the brominated tungsten atoms, and at $\delta = -123.1$ ppm for the tungsten atoms in the W_3 cap. The replacement of terminal oxygen atoms (O_t) by bromine shifts the resonance signal of the brominated tungsten atoms significantly downfield (+189.1 ppm); the more terminal oxygen atoms which are replaced, the greater the signal shifts (+281.6 ppm for WBr_2 in $[W_2O_4Br_4(\mu\text{-}C_2O_4)]^{2-}$). Similar shifts occurred in the case of replacement of O_t by chlorine [58]. In contrast to these, fluoride substituted polyoxotungstates $HW_{12}O_{40-x}F_x^{n-}$, x = 1–3 and $H_2W_{12}O_{40-x}F_x^{n-}$ x = 1, 2, where F^- replaces the oxygen atoms of the internal tetrahedron XO_4, exhibited little deshielding of the tungsten atoms (Table 6). Because the replacement of F^- slightly lowers the symmetry of the whole anion the single line in the ^{183}W NMR spectrum of the parent anion $H_2W_{12}O_{40}^{6-}$ split into three lines [112].

Table 6
Chemical shifts of $HW_{12}O_{40-x}F_x^{n-}$ and $H_2W_{12}O_{40-x}F_x^{n-}$ [111]

x	Chemical shift (δ) in ppm
$HW_{12}O_{40-x}F_x^{n-}$	
1	−130, −115, −107
2	−110, −103, −97
3	−106, −90
$H_2W_{12}O_{40-x}F_x^{n-}$	
0	−111
1	−109, −105, −95
2	−100, −83, −85

The replacement of the coordinated water molecule in $Li_6PW_{11}Ru(H_2O)O_{39}$ by dimethyl sulfoxide or by maleic acid results in a small shift of the signal of the W atoms adjacent to the substituted atom. This can be interpreted in terms of a competition for the Ru π-electrons between the tungstophosphate and other acceptor ligands [102].

3.5.3. Counterion and solvent

Some researchers indicated that tungsten-183 chemical shifts are counterion-dependent [12,13,22,36,44,45,51,85]. Table 7 illustrates some examples. Surveying the data in Table 7, the resonance lines shift downfield as the counterion size increases. Canny et al. [22] indicated that this is consistent with a modification of the distribution of the negative charges on all the oxygen atoms of the structure when a M^+ cation substitutes another M^+ cation. Another explanation is a stronger association of Li^+ with polyanions, as compared with Na^+ [13].

3.6. 2-D NMR spectroscopy

In more complex coupling problems the similarity of $^2J_{W–O–W}$ values may produce ambiguity in determination of connectivity. In principle, any ^{183}W can have up to 4 different adjacent ^{183}W atoms. Furthermore, the lower intensity of satellite lines make them difficult to differentiate from major lines of slight impurities, and the line broadening (up to ∼54 Hz) caused by displacement of quadrupolar nuclide or by presence of vacancies leads even to the disappearance of some resonances [17,26,45]. These problems prompted Brevard et al. [47] and Domaille et al. [54] to introduce two-dimensional (2-D) NMR techniques (2-D INADEQUATE and 2-D COSY) for establishing connectivity

Table 7
Chemical shifts with different cations

Polyanion	M^+	Solvent	Chemical shift (δ) in ppm (intensity ratio)	References
α-$SiW_{11}O_{39}^{8-}$	Na	D_2O	−100.8, −116.1, −121.3, −127.9, −143.2, −176.1 (2:2:1:2:2:2)	[29,47]
	Li		−105.2, −106.0, −120.5, −121.6, −143.5.−173.5 (2:2:1:2:2:2)	[56]
α-$PW_{11}O_{39}^{7-}$	Na	D_2O	−97.3, −102, −108.9, −116.6, −132.0, −152.1 (1:2:2:2:2:2)	[47]
	Li		−98.1, −98.8, −103.6, −121.4, −132.4, −152.2 (1:2:2:2:2:2)	
α_2-$P_2W_{17}O_{61}^{10-}$	K	D_2O	−127.9, −140.8, −159.6, −175.8, −179.6, −218.9, −222.7, −225.0, −242.3 (2:2:2:1:2:2:2:2:2)	[56]
	TBA[a]	DMSO–D_2O	−93.6, −112.2, −123.7, −156.4, −174.9, −177.8, −180.9, −183.4, −189.3 (2:1:2:2:2:2:2:2:2)	[56]
α-$PW_{12}O_{40}^{3-}$	TBA	S[b]	−86.7	[45]
α-$SiW_{12}O_{40}^{4-}$	TBA		−92.1	[45]
γ-$SiW_{10}O_{36}^{8-}$	Li	D_2O	−106.9, −147.9, −163.6	[22]
	Na		−102.3, −143.8, −162.8	
	K		−96.4, −137.2, −158.2	

[a] TBA = $(C_4H_9)_4N$.
[b] S = DMF–CD_3CN.

between tungsten atoms. The major advantage of the 2-D NMR method is that it is unnecessary to accurately measure the $^2J_{W-O-W}$ values to establish the connectivity; the scalar coupling merely carries the chemical shift correlations for coupled sites, and the differentiation is achieved on the basis of single- or double-quantum frequencies [26]. 2-D ^{183}W NMR methods have been successfully used in establishing the structures of substituted species [25,28,38,47,54,55].

Sveshnikov and Pope [113] developed a method for assignment of the multiline tungsten-183 NMR spectra of diamagnetic polyoxotungstates from intensity patterns which may be used in cases where the ^{183}W–^{183}W satellites are not clearly observable or resolved from the central line.

4. ^{183}W NMR in the study of POMs

4.1. Detecting the formation of new species and their purity

Structural characterization of polyoxotungstates in solution is based on three properties of the tungsten-183 spectrum: spectral envelope, relative intensity of the lines and homonuclear and heteronuclear coupling constants. As seen in the text earlier, complexes with the same symmetry and similar anionic structure exhibit identical spectral envelope and therefore new species with different substituted elements can be established in solution by the spectral envelope. Many tungsten-183 NMR spectra were recorded for identification of the formation of new species and their purity (some references mentioned earlier, and [114–122]). Further structural characterization or determination of the W–W connectivity requires an accurate measurement of coupling constants $^2J_{W-O-W}$ and then the use of the rule that Lefebvre et al. [19] found or 2-D ^{183}W NMR techniques.

4.2. Structural characterization of POMs in solution

4.2.1. Inference of new structure

Himeno et al. [35] recorded the ^{183}W NMR spectrum of the *n*-Pr_4N^+ salt of anion $[H_6W_{18}O_{60}]^{6-}$ saturated in propylene carbonate in order to characterize structurally the complex. The ^{183}W NMR spectrum consisted of three lines at −122.0, −146.6 and −161.1 ppm with the intensity ratio of 1:1:1, indicating that the $[H_6W_{18}O_{60}]^{6-}$ complex contains three groups of six structurally equivalent W atoms. On this basis, a possible structure seems to contain two six-membered rings of WO_6 octahedra capped on opposite sides by two corner-shared W_3O_{12} groups in which the six capping W atoms are structurally equivalent.

Mayer and Thouvenot [123] inferred the structure of the hybrid anion $[A\text{-}PW_9O_{34}(RPO)_2]^{5-}$ from multinuclear (^{31}P, ^{183}W) NMR studies. The five line spectrum of $[PW_9O_{34}(RPO)_2]^{5-}$ (−42.8, −94.6, −140.0, −189.0, −193.8 with intensity ratio 1:2:2:2:2 for Et_4N^+ salt in DMF-$(CD_3)_2CO$) indicated a lowering of the symmetry of the tungstophosphate framework from C_{3v} to C_s. The reason for this is that two RPO groups were linked asymmetrically to the PW_9 moiety. The line with intensity one was assigned first to W1 in triplet (see figures in [123]) based on four possible structures. By using ^{31}P decoupling spectrum two $^2J_{W-O-W}$ values (7.3 and 24.4 Hz) of this line were measured and then the W atoms linked with W1 were determined, edge-shared W2 and W3 in the triplet and two W atoms in the six-membered belt. Three of four broad lines had nearly same coupling constant (24–25 Hz) and made it impossible to assign the lines to W sites. They utilized the heteronuclear coupling constants $^2J_{W-O-P}$. The resonances of the tungsten atoms connecting with the RPO group appear as doublets of doublets due to the heteronuclear coupling with the phosphorus atom of the PW_9O_{34} moiety ($^2J_{W-O-P} \approx 2$ Hz) and that of one RPO group ($^2J_{W-O-P} \approx 6$–9 Hz). The two such resonances were

assigned to the four tungsten atoms connecting to the RPO groups. Combining the large $^2J_{W-O-W}$ values the remaining resonances were assigned to the two tungsten atoms not connecting with the RPO group.

4.2.2. Geometry

The ^{183}W NMR spectrum may yield information about subtle changes in symmetry of complexes. Bartis et al. [29] found in studying $[Ln(SiW_{11}O_{39})_2]^{13-}$ and $[Ln(P_2W_{17}O_{61})_2]^{17-}$ that two coordinated anions with Ln = La had six lines and nine lines, respectively, corresponding to C_{2v} and C_2 symmetry; and those with Ln = Lu, Yb had 11 lines and 15 lines, showing the reduced symmetry of those anions. They explained that the small size of the heavier lanthanides resulted in a disorder of square anti-prism and therefore a reduction of symmetry.

4.3. Distinguishing isomers

Contant and Thouvenot [20] proposed a criterion for distinguishing isomers. The difference between chemical shifts of polar atoms and belt atoms in the α-PW_9 group of α-$[P_2W_{18}O_{62}]^{6-}$, $\Delta\delta = 172 - 126.5 = 45.5$ ppm while that in the β-PW_9 group of β- and γ-$[P_2W_{18}O_{62}]^{6-}$, has $\Delta\delta = 80$ ppm. Recently, Contant et al. [34] assigned the α-structure to the new complex octadecatungstomonophosphate based on the difference $\Delta\delta = 181.3 - 144.9 = 36.4$ ppm between the two chemical shifts of the PW_9 group in $[H_4PW_{18}O_{62}]^{7-}$ (the two lines with an observed heteronuclear coupling $^2J_{W-O-P}$ were attributed to the half-anion PW_9 and the other two signals at −127.8 ppm (6W) and −135.7 ppm (3W) without heteronuclear coupling were attributed to half-anion H_nW_9). Mbomekalle et al. [116] found the difference between two chemical shifts in the AsW_9 group in $[H_4AsW_{18}O_{62}]^{7-}$ ($\Delta\delta = 161.3 - 134.6 = 26.7$ ppm) was fairly close to that in the corresponding half-anion in α-$[As_2W_{18}O_{62}]^{6-}$ ($\Delta\delta = 142.8–120.1 = 22.7$ ppm), while the difference in β- or γ-$[As_2W_{18}O_{62}]^{6-}$ is close to 54 ppm [20]. Anion $[H_4AsW_{18}O_{62}]^{7-}$ was assigned to the α-structure.

Meng et al. proposed a similar method to distinguish the α-isomer from the β-isomer of $XW_9M_3O_{40}^{n-}$ [63]. Domaille et al. [54] determined the structure of $PTi_2W_{10}O_{40}^{7-}$. Five isomers can be formed in the reaction of NaH_2PO_4, Na_2WO_4 and $TiCl_4$. Two of them have C_s symmetry, one with C_2 symmetry, one with C_{2v} symmetry and the last has C_1 symmetry. Their the ^{183}W NMR spectral envelope could be expected theoretically based on the symmetries: C_s symmetry, six lines (intensity ratio 2:2:2:2:1:1); C_2 symmetry, five lines (intensity ratio 2:2:2:2:2); C_{2v} symmetry, three lines (intensity ratio 4:4:2); C_1 symmetry, nine distinguishable lines. The five isomers can be distinguished principally based on the spectral envelope and the intensity ratio. The comparison of experimental spectra with those predicted favored the isomer with C_2 symmetry, that is, the product that they obtained was 1, 4-$PTi_2W_{10}O_{40}^{7-}$. Later, Domaille [27] verified the structures of mono-substituted Keggin anion $XW_{11}V$ (X = Si, P, B) by using 2-D INADEQUATE ^{183}W NMR technique and the structure of bi-substituted Keggin anions α-1,2-XV_2W_{10} (X = Si, P) by combining the results of 2-D INADEQUATE ^{183}W NMR spectra and 1-D $^{183}W\{^{51}V\}$ NMR spectra as well as ^{51}V NMR spectra. The tri-substituted Keggin anions A-α-1,2,3-$XW_9V_3O_{40}^{7-}$ (X = Si, P), A-β-1,2,3-$SiW_9V_3O_{40}^{7-}$ were solved by using the coupling constants ($^2J_{W-O-W} = 15.7 \pm 1.2$ Hz) and the simple line pattern (two lines with intensity ratio of 2:1). The lines are relatively sharp due to edge-sharing of vanadium and tungsten and the rapid relaxation of the ^{51}V nuclei.

4.4. Miscellaneous

NMR is also a very valuable tool to study the electron density distribution due to the large chemical shifts induced both by paramagnetic atoms and by electron transfer between atoms in diamagnetic POM. The regions where the additional electrons reside in the diamagnetic reduced anions can be identified directly by determining the relaxation time T_1. The ^{183}W NMR spectrum also can elucidate the effects of the additional electrons on neighboring atoms. Kozik et al. [108] determined the T_1 of W nuclides in a study of the ESR-silent heteropoly blue (reduced POM). They found an inverse correlation between chemical shifts and relaxation times, that is, the relaxation times decreased with increasing of the electron density of the nuclide under consideration. Based on the chemical shifts and relaxation times, they indicated the regions of electron delocalization of the reduced species α-$SiW_{12}O_{40}^{6-}$, $P_2W_{18}O_{62}^{8-}$, α-$P_2Mo_3W_{15}O_{62}^{8-}$. Duncan and Hill [12] and Tézé et al. [24] reported similar work on diamagnetic two-electron reduced species.

Although ^{183}W NMR spectroscopy has played an important role in the study of POMs, there are some limits to its application. The ^{183}W NMR spectrum of unstable or metastable POM in solution cannot be detected due to its longer acquisition time, and as a means of monitoring the progress of reaction ^{183}W NMR spectroscopy is less suitable than ^{31}P NMR spectroscopy. Furthermore, in some cases, the ^{183}W NMR spectrum cannot discriminate between monomeric and polymeric solute species or a mixture of both under fast exchange condition [81,101,122].

5. Theoretical studies of the ^{183}W NMR spectra

Kazansky et al. [124] have carried out extended Hückel molecular orbital (EHMO) calculations using cluster approach to polyoxo anions for a single MO_6 octahedron of various symmetry, and based on the results they have analyzed ^{183}W and ^{17}O NMR spectra. Inoue et al. [125] have analyzed the ^{183}W NMR and UV spectra of the polyoxotungstates by extended Hückel molecular orbital calculations. The calculated HOMO–LUMO separations for $LaW_{10}O_{36}^{9-}$, $Ce^{IV}W_{10}O_{36}^{8-}$, $W_{10}O_{32}^{4-}$ and $W_6O_{19}^{2-}$

correspond to the wavelengths of the lowest charge transfer band observed in UV spectra of aqueous solutions.

The ab initio and DFT calculation of nuclear shielding provides an attractive method for structure elucidation, since it should yield an independent estimate of the chemical shift which can then: (a) be used to predict the spectral region in which an NMR signal can be found; and (b) ultimately serve for spectral assignment through the comparison with experimental values. Bagno and co-workers [126,127] carried out an effective core potential DFT calculations of nuclear shielding of tungsten complexes taking relativistic effects into account by means of the zero-order regular approximation (ZORA), including mononuclear complexes, WS_4^{2-}, WF_4O, WF_6, etc. which span the whole known shielding range, and polyoxotungstates, $V_nW_{6-n}O_{19}^{(2+n)-}$, $n = 0$–2; $W_{10}O_{32}^{4-}$, α-$PW_{11}O_{39}^{7-}$, α-$PRu(H_2O)W_{11}O_{39}^{7-}$, α-$PW_{12}O_{40}^{3-}$. The results [125] show a good linear relationship spanning ca. 8000 ppm between calculated and experimental ^{183}W shifts for mononuclear complexes. The α-$PW_{12}O_{40}^{3-}$ fits well in the relationship. In this work, they also examined the relationship between chemical shifts and atomic charge and indicated that negatively charged W nuclei are deshielded, in agreement with an empirical model [16]. In another study [126] they gave a formula: $\delta_{cal} = a\delta_{exp} + b$, and used the results obtained from $V_nW_{6-n}O_{19}^{(2+n)-}$ and $W_{10}O_{32}^{4-}$ to estimate the shifts of the structurally related but elusive anion $W_5O_{18}^{6-}$: $\delta = 96$ and 8.6 ppm for the equatorial and axial tungsten nuclei, respectively. The data fall within the range found for similar species such as $Ce(W_5O_{18})_2^{9-}$, $\delta = 149.1$ and 51.5 ppm. Considering the effect of the counterion on chemical shift they compared the calculated and experimental values for lacunary α-$PW_{11}O_{39}^{7-}$ anion as isolated anion and α-$LiPW_{11}O_{39}^{8-}$ complex, and found that the overall ordering of the calculated six signals for α-$LiPW_{11}O_{39}^{8-}$ fits the experimental spectrum much better although the W4 atoms adjacent to the lacuna and in a plenary triplet are strongly deshielded. The calculated spectrum for α-$PRu(DMSO)W_{11}O_{39}^{5-}$ gave a same ordering of signals, except for W5 and W6. All calculated results indicate that the DFT calculation for ^{183}W nuclear shielding may predict the shift range and assignment of the spectra of polyoxotungstates.

6. Conclusion

Three properties of the tungsten-183 spectrum, spectral envelope, relative intensity of the lines and homonuclear and heteronuclear coupling constants, are the bases for the structural characterization of polyoxotungstates in solution. As seen in the text above, the complexes with the same symmetry and similar anionic structure exhibit identical spectral envelope and therefore new species with different substituted elements can be established in solution by the spectral envelope. Although the majority of the NMR spectra were recorded for the purpose of identification of new species, ^{183}W NMR spectroscopy plays an important role in the verification of new anionic structures, to distinguish isomers in solution as well as to monitor the progress of reaction. ^{183}W NMR spectroscopy can provide valuable structural information when a high quality crystal cannot be obtained and X-ray single crystal diffraction method is hampered. Theoretical analyses of the ^{183}W chemical shift have begun to appear in the literature to explore the influence of environment on electron population on the W atom under consideration. The further development of theory and instrumentation will make ^{183}W NMR spectroscopy even more effective.

Acknowledgements

This work was supported by the Chinese National Science Fund (39970842).

References

[1] M.P. Klein, J. Happe, Bull. Am. Phys. Soc. 6 (1961) 104.
[2] J. Banck, A. Schwenk, Z. Phys. B 20 (1975) 75.
[3] W. McFarlane, A.M. Noble, J.M. Winfield, J. Chem. Soc., Dalton Trans. (1971) 984.
[4] H.C.E. McFarlane, W. McFarlane, D.S. Rycroft, J. Chem. Soc., Dalton Trans. (1976) 1616.
[5] G.T. Andrews, I.J. Colquhoun, W. McFarlane, S.O. Grim, J. Chem. Soc., Dalton Trans. (1982) 2353.
[6] R. Acerete, C.F. Hammer, L.C.W. Baker, J. Am. Chem. Soc. 101 (1979) 267.
[7] M.T. Pope, Heteropoly and Isopoly Oxometalates, Springer-Verlag, New York, 1983.
[8] D.E. Katsoulis, Chem. Rev. 98 (1998) 359.
[9] N. Mizuno, M. Misono, Chem. Rev. 98 (1998) 199.
[10] I.V. Kozhevnikov, Chem. Rev. 98 (1998) 171.
[11] J.T. Rhule, C.L. Hill, D.A. Judd, Chem. Rev. 98 (1998) 327.
[12] D.C. Duncan, C.L. Hill, Inorg. Chem. 35 (1996) 5828.
[13] R.I. Maksimovskaya, K.G. Burtseva, Polyhedron 4 (1985) 1559.
[14] J.J. Dechter, Prog. Inorg. Chem. 33 (1985) 429.
[15] C.J. Jameson, J. Mason, in: J. Mason (Ed.), Multinuclear NMR, Plenum Press, New York, 1987.
[16] C.J. Jameson, H.S. Gutowsky, J. Chem. Phys. 40 (1964) 1714.
[17] R. Acerete, C.F. Hammer, L.C.. Baker, J. Am. Chem. Soc. 104 (1982) 5384.
[18] R. Acerete, N. Casan-Pastor, J. Bas-Serra, L.C.W. Baker, J. Am. Chem. Soc. 111 (1989) 6049.
[19] F. Lefebvre, F. Chauveau, P. Doppelt, C. Brevard, J. Am. Chem. Soc. 103 (1981) 4589.
[20] R. Contant, R. Thouvenot, Inorg. Chim. Acta 212 (1993) 41.
[21] R. Contant, G. Hervé, R. Thouvenot, Presented at the CNRS-NSF Workshop on Polyoxometalates, Saint-Lambert des Bios, France, 1983.
[22] J. Canny, A. Tézé, R. Thouvenot, R. Contant, G. Hervé, Inorg. Chem. 25 (1986) 2114.
[23] R. Thouvenot, A. Tézé, R. Contant, G. Hervé, Inorg. Chem. 27 (1988) 524.
[24] A. Tézé, J. Canny, L. Gunban, et al., Inorg. Chem. 35 (1996) 1001.
[25] E. Cadon, R. Thouvenot, A. Tézé, G. Hervé, Inorg. Chem. 31 (1992) 4128.
[26] L.P. Kazansky, Chem. Phys. Lett. 223 (1994) 289.

[27] P.J. Domaille, J. Am. Chem. Soc. 106 (1984) 7677.
[28] M.A. Fedotov, B.Z. Pertisikov, D.K. Damovich, Polyhedron 9 (1990) 1249.
[29] J. Bartis, S. Sukal, M. Donkova, E. Kraft, R. Kronzon, M. Blumstein, L.C. Francesconi, J. Chem. Soc., Dalton Trans. (1997) 1937.
[30] R.G. Finke, B. Rapko, C.L. Weakley, Inorg. Chem. 28 (1989) 1573.
[31] R.G. Finke, M. Droege, J.R. Hutchinson, et al., J. Am. Chem. Soc. 103 (1981) 1587.
[32] R. Acerete, S. Harmalker, C.F. Hammer, M.T. Pope, L.C.W. Baker, J. Am. Chem. Soc. 101 (1979) 777.
[33] R. Acerete, C.F. Hammer, L.C.W. Baker, Inorg. Chem. 24 (1984) 1478.
[34] R. Contant, S. Piro-Sellem, J. Canny, R. Thouvenot, Comput. R. Acad. Sci. Ser. IIC 3 (2000) 157.
[35] S. Himeno, M. Yoshihara, M. Maekawa, Inorg. Chem. Commun. 4 (2001) 5.
[36] J. Bartis, Y. Kanina, M. Blumenstein, et al., Inorg. Chem. 35 (1996) 1497.
[37] J. Gong, L.-Y. Qu, Y.-G. Chen, Chin. Inorg. Chem. 11 (1995) 102.
[38] T.L. Jorris, M. Kozik, N. Casan-Pastor, P.J. Domaille, R.G. Finke, W.K. Miller, L.C.W. Baker, J. Am. Chem. Soc. 109 (1987) 7402.
[39] R. Contant, R. Thouvenot, Can. J. Chem. 69 (1991) 1498.
[40] A. Ostuni, M.T. Pope, Comput. R. Acad. Sci. Ser. IIC 3 (2000) 199.
[41] R.G. Finke, B. Ropko, R.J. Saxton, et al., J. Am. Chem. Soc. 108 (1986) 2947.
[42] R.G. Finke, M. Droege, Inorg. Chem. 22 (1983) 1006.
[43] D.A. Judd, Q. Chen, C.F. Campann, C.L. Hill, J. Am. Chem. Soc. 119 (1997) 5641.
[44] P.A. Lorenzo-Lwis, P. GiDi, A. Sanclez, et al., Transition Met. Chem. 24 (1999) 686.
[45] O.A. Gansow, R.K.C. Ho, W.C. Klemperer, J. Organomet. Chem. 187 (1980) C27.
[46] T. Yamase, T. Usami, J. Chem. Soc., Dalton. Trans. (1988) 185.
[47] C. Brevard, R. Schimpf, G. Touné, C.M. Tourné, J. Am. Chem. Soc. 105 (1983) 7059.
[48] J.J. Hastings, O.W. Howarth, Polyhedron 12 (1993) 847.
[49] E. Radokv, R.H. Beer, Polyhedron 14 (1995) 2139.
[50] Y.-G. Chen, Zh.-P. Zhu, H.-D. Wu, et al., Chin. Inorg. Chem. 15 (1999) 205.
[51] A. Proust, M. Fournier, R. Thouvenot, P. Gouzerh, Inorg. Chim. Acta 215 (1994) 619.
[52] X. Wei, M.H. Dichman, M.T. Pope, Inorg. Chem. 36 (1997) 130.
[53] W.H. Knoth, P.J. Domaille, D.C. Roe, Inorg. Chem. 22 (1983) 198.
[54] P.J. Domaille, W.H. Knoth, D.C. Roe, Inorg. Chem. 22 (1983) 818.
[55] M.A. Fedotov, L.G. Detusheva, L.I. Kuznetsova, V.A. Likholobov, Zh. Neorg. Khim. 38 (1992) 515.
[56] R.D. Peacoke, T.J.R. Weakley, J. Chem. Soc. A (1971) 1836.
[57] M. Sadakane, M.H. Dickman, M.T. Pope, Angew. Chem. Int. Ed. 39 (2000) 2914.
[58] R.J. Errington, R.L. Wingod, W. Clegg, M.R.J. Elsegood, Angew. Chem. Int. Ed. 39 (2000) 3884.
[59] Y.-G. Chen, L.-Y. Qu, J. Peng, M. Yu, Chem. Res. Chin. Univ. 9 (1993) 6.
[60] B. Rapko, M. Pohl, R.G. Finke, Inorg. Chem. 33 (1994) 3625.
[61] J. Liu, F. Ortega, P. Sethuraman, D.E. Katsulis, C.E. Costello, M.T. Pope, J. Chem. Soc., Dalton Trans. (1992) 1901.
[62] F. Xin, M. Pope, J. Am. Chem. Soc. 118 (1997) 5531.
[63] L. Meng, X.-P. Zhan, M. Wang, J.-F. Liu, Polyhedron 20 (2001) 881.
[64] F. Xin, M.T. Pope, G.J. Long, U. Russo, Inorg. Chem. 35 (1996) 1207.
[65] K. Nomiya, C. Nozaki, A. Kano, T. Taguchi, K. Ohsawa, J. Organomet. Chem. 533 (1997) 153.
[66] G.S. Kim, H. Zeng, D. VanDerveer, C.L. Hill, Angew. Chem. Int. Ed. 38 (1999) 3205.
[67] Y. Lin, T.J.R. Weakley, B. Rapko, R.G. Finke, Inorg. Chem. 32 (1993) 5095.
[68] R.G. Finke, M.W. Droege, J. Am. Chem. Soc. 106 (1984) 7274.
[69] T. Yamase, T. Ozeki, H. Sakamoto, S. Nishiya, A. Yamamoto, Bull. Chem. Soc. Jpn. 66 (1993) 103.
[70] W.H. Knoth, Organometallics 4 (1985) 62.
[71] A. Botar, B. Botar, P. Gili, A. Muller, J. Meyer, H. Bogge, M. Schmidtmann, Anorg. Allg. Chem. 622 (1996) 1435.
[72] W.H. Knoth, P.J. Domaille, R.L. Harlow, Inorg. Chem. 25 (1986) 1577.
[73] L.I. Kuanetsova, N.I. Kuznetsova, L.G. Detusheva, M.A. Fedotov, V.A. Likholobov, J. Mol. Catal. A 158 (2000) 429.
[74] H.T. Evans, C.M. Tourné, G.F. Tourné, T.J.R. Weakley, J. Chem. Soc., Dalton Trans. (1986) 2699.
[75] C.M. Tourné, G.F. Tourné, F. Zonnevijlle, J. Chem. Soc., Dalton Trans. (1991) 143.
[76] M. Abessi, R. Contant, R. Thouvenot, G. Hervé, Inorg. Chem. 30 (1991) 1695.
[77] J. Bartis, M. Dankova, J.J. Lessmann, W.DeW. Horrocks Jr., L.C. Francesconi, Inorg. Chem. 38 (1999) 1042.
[78] A. Venturelli, A. Smirnoff, M. Nilges, R.L. Belford, L.C. Francesconi, J. Chem. Soc., Dalton Trans. (1999) 301.
[79] M.R. Antonio, L. Soderholm, G. Jennings, L.C. Francesconi, M. Dankova, J. Bartis, J. Alloys Compd. 275–277 (1998) 827.
[80] K. Nomuya, C. Nozaki, M. Kaneko, R.G. Finke, M. Pohl, J. Organomet. Chem. 505 (1995) 23.
[81] K. Nomiya, Y. Arai, Y. Shimizu, M. Takahashi, T. Takayama, H. Weiner, T. Nagata, J.A. Widegren, R.G. Finke, Inorg. Chim. Acta 300–302 (2000) 285.
[82] D.J. Edlund, R.J. Saxton, D.K. Lyon, R.G. Finke, Organometallics 7 (1988) 1692.
[83] M.A. Fedotov, L.P. Kazansky, V.I. Spitsyn, Dokl. Akad. Nauk. SSSR 272 (1983) 1179.
[84] L.-H. Bi, E.-B. Wang, J. Peng, et al., Inorg. Chem. 39 (2000) 671.
[85] A. Chemseddine, C. Sanchez, J. Livage, J.P. Launay, M. Fournier, Inorg. Chem. 2 (1984) 2609.
[86] M.A. Fedotov, E.P. Samokhvalova, L.P. Kazansky, Polyhedron 15 (1996) 2241.
[87] L. Bartis, M. Dankova, L.C. Francesconi, M. Blumenstein, J. Alloys Compd. 249 (1997) 56.
[88] M.A. Fedotov, E.P. Samokhvallova, L.P. Kazansky, Koordin. Khim. 22 (1996) 219.
[89] A. Proust, R. Thouvenot, S.-G. Roh, Inorg. Chem. 34 (1995) 14106.
[90] V.W. Day, W.G. Klemperer, C. Schwartz, J. Am. Chem. Soc. 109 (1987) 6030.
[91] I. Creaser, M.C. Hechel, R.J. Neitz, M.T. Pope, Inorg. Chem. 32 (1993) 1573.
[92] M. Alizadeh, S.P. Harmalker, Y. Jeannin, J. Martin-Frere, M.T. Pope, J. Am. Chem. Soc. 107 (1985) 2662.
[93] E. Cadot, V. Béreau, B. Marg, S. Halut, F. Sécheresse, Inorg. Chem. 35 (1996) 3099.
[94] R. Thouvenot, M. Michelon, A. Tézé, G. Hervé, in: M.T. Pope, A. Müller (Eds.), Polyoxometalates. From Platonic Solids to Anti-Retroviral Activity, Kluwer Academic Publishers, Dordrecht, 1994, p. 184.
[95] M. Leyrie, G. Hervé, Nouv. J. Chim. 2 (1978) 223.
[96] J. Liu, J. Guo, B. Zhao, G. Xu, M. Li, Transition Met. Chem. 18 (1993) 205.
[97] J.-F. Liu, Y.-G. Chen, L. Meng, L. Guo, J. Liu, M.T. Pope, Polyhedron 17 (1998) 1541.
[98] K. Wasssermann, M.T. Pope, Inorg. Chem. 40 (2001) 2763.
[99] K.-C. Kim, M.T. Pope, J. Chem. Soc., Dalton Trans. (2001) 986.
[100] K.-C. Kim, M.T. Pope, J. Am. Chem. Soc. 121 (1999) 8512.
[101] M. Sadakane, M.H. Dickman, M.T. Pope, Inorg. Chem. 40 (2001) 2715.
[102] C. Rong, M.T. Pope, J. Am. Chem. Soc. 114 (1992) 293.

[103] A. Bagno, M. Bonchio, A. Sartorel, G. Scorrano, Eur. J. Inorg. Chem. (2000) 17.
[104] L.P. Kazansky, B.R. McGarvey, Coord. Chem. Rev. 188 (1999) 157.
[105] M. Fournier, C. Rocchiccioli-Deltcheff, L.P. Kazansky, Chem. Phys. Lett. 223 (1994) 629.
[106] N. Casan-Pastor, P. Gomez-Romero, C.B. Jameson, L.C.W. Baker, J. Am. Chem. Soc. 113 (1991) 5658.
[107] M. Kozik, M.T. Pope, in: M.T. Pope, A. Muller (Eds.), Polyoxometalates. From Platonic Solids to Anti-Retroviral Activity, Kluwer Academic Publishers, Dordrecht, 1994, p. 191.
[108] M. Kozik, C.F. Hammer, L.C.W. Baker, J. Am. Chem. Soc. 108 (1986) 2748.
[109] N. Casan-Pastor, L.C.W. Baker, in: M.T. Pope, A. Muller (Eds.), Polyoxometalates. From Platonic Solids to Anti-Retroviral Activity, Kluwer Academic Publishers, Dordrecht, 1993, p. 203.
[110] K. Piepgrass, M.T. Pope, J. Am. Chem. Soc. 109 (1987) 1586.
[111] K. Piepgrass, M.T. Pope, J. Am. Chem. Soc. 111 (1989) 753.
[112] L.P. Kazansky, J. Chim. Phys. 91 (1994) 341.
[113] N.N. Sveshnikov, M.T. Pope, Inorg. Chem. 39 (2000) 591.
[114] R.L. Kravchenko, M.A. Fedotov, R.I. Maksimovskaya, L.I. Kuznetsova, Zh. Neorg. Khim. 39 (1994) 629.
[115] X. Wang, J. Liu, J. Li, J. Liu, Inorg. Chem. Commun. 4 (2001) 302.
[116] M. Mbomekalle, B. Keita, L. Nadjo, R. Contant, N. Belai, M.T. Pope, Inorg. Chim. Acta 342 (2003) 219.
[117] Q.-Y. Wu, Sh.-K. Wang, D.-N. Li, X.-F. Xie, Inorg. Chem. Commun. 5 (2002) 308.
[118] E. Cadot, V. Béreau, F. Sécheresse, Inorg. Chim. Acta 252 (1996) 101.
[119] C. Raţiu, A.-R. Tomşa, A. Koutsodimou, P. Falaras, T. Budiu, Polyhedron 21 (2002) 353.
[120] N. Belai, M. Sadakane, M.T. Pope, J. Am. Chem. Soc. 123 (2001) 2087.
[121] T. Yamase, T. Ozeki, S. Motomura, Bull. Chem. Soc. Jpn. 65 (1992) 1453.
[122] O.A. Kholdeeva, C.M. Maksimov, R.I. Maksimovskaya, L.A. Kovaleva, M.A. Fedotov, V.A. Grigoriev, C.L. Hill, Inorg. Chem. 39 (2000) 3828.
[123] C.R. Mayer, R. Thouvenot, J. Chem. Soc., Dalton Trans. (1998) 7.
[124] L.P. Kazansky, P. Chaquin, M. Fournier, G. Hervé, Polyhedron 17 (1998) 4353.
[125] M. Inoue, T. Yamase, L.P. Kazansky, Polyhedron 22 (2003) 1183.
[126] A. Bagno, M. Bonchio, Chem. Phys. Lett. 317 (2000) 123.
[127] A. Bagno, M. Bonchio, A. Sartorel, G. Scorrano, Chem. Phys. Chem. 4 (2003) 517.